New Phytologist

The mirror crack'd: both pigment and structure contribute to the glossy blue appearance of the Mirror Orchid, *Ophrys speculum*

Silvia Vignolini[1,2], Matthew P. Davey[1], Richard M. Bateman[3], Paula J. Rudall[3], Edwige Moyroud[1], Julia Tratt[3], Svante Malmgren[4], Ullrich Steiner[2], and Beverley J. Glover[1*]

[1]Department of Plant Sciences, University of Cambridge, Downing Street, Cambridge, CB2 3EA, UK

[2]Department of Physics, Cavendish Laboratory, University of Cambridge, J. J. Thomson Avenue, Cambridge, CB3 0HE, UK

[3]Jodrell Laboratory, Royal Botanic Gardens Kew, Richmond, Surrey, TW9 3AB, UK

[4]Radagatan 8, SE 531-52, Lidköping, Sweden

[*]For correspondence: telephone, +44 (0)1223 333938, email bjg26@cam.ac.uk

RUNNING HEAD: *Structure enhances colour in the Mirror Orchid*

Total word count: 5112

Includes 6 figures and 2 tables

Summary

– The Mediterranean orchid genus *Ophrys* is remarkable for its pseudo-copulatory pollination mechanism; naïve male pollinators are attracted to the flowers by olfactory, visual and tactile cues. The most striking visual cue is a highly reflective, blue speculum region at the centre of the labellum, which mimics the corresponding female insect and reaches its strongest development in the Mirror Orchid, *O. speculum*.

– We explored the structure and properties of the much-discussed speculum by scanning and transmission electron microscopic examination of its ultrastructure, visible and ultraviolet (UV) angle-resolved spectrophotometry of the intact tissue, and mass spectrometry of extracted pigments.

– The speculum contrasts with the surrounding labellar epidermis in being flat-celled with a thick, smooth cuticle. The speculum is extremely glossy, reflecting intense white light in a specular direction, but at more oblique angles it predominantly reflects blue and UV light. Pigments in the speculum, dominantly the cyanidin 3-(3”-malonylglucoside), are less diverse than in the surrounding regions of the labellar epidermis and lack quercetin co-pigments.

– Several physical and biochemical processes interact to produce the striking and much-discussed optical effects in these flowers, but the blue colour is not produced by structural means and is not iridescent.

Key words: anthocyanin, co-pigmentation, epidermis, labellum, *Ophrys speculum*, pollinator deceit, specular reflection, structural colour.

Introduction

The Mirror Orchid

The morphological distinctiveness, complexity and commercial importance of orchid flowers have promoted them to popular models for studies of floral development, functional morphology, reproductive biology and plant–pollinator interactions. The genus *Ophrys* is well-suited for study in each of these disciplines, and particularly for analysis of the interface between floral morphology and pollinator attraction.

The floral bauplan of *Ophrys* is typical of most species of the subfamily Orchidoideae, which includes most of the European terrestrial orchids (Rudall & Bateman 2002). Stamen and pistils are congenitally fused into a gynostemium wherein the single fertile stamen bears two anther locules, each containing a club-shaped pollinarium with an adhesive viscid disc at the proximal end linked to a pollen mass (pollinium) toward the distal end. The stigmatic surface is located immediately below the viscid discs. The inferior ovary is rich in minute ovules. The perianth consists of two closely-spaced whorls each composed of three organs, the three petals being located immediately distal to the three sepals. The lower median petal, termed the labellum, is often larger and usually more complex than the lateral petals. The resulting floral morphology, showing unusually strong bilateral symmetry, was recognized by Darwin (1862) as strongly encouraging transfer of pollinaria between inflorescences to facilitate cross-pollination.

The bilateral symmetry of the orchid flower, and morphological complexity of the labellum, are especially strongly expressed in the genus *Ophrys* (Fig. 1A). A comparative overview of the genus by Bradshaw *et al*. (2010) demonstrated that this complexity extends to the micromorphological scale, revealing a wide range of epidermal cell types located in specific

68 regions of the labellum and presumably reflecting its unusual pseudocopulatory mode of
69 pollination. Most *Ophrys* species attract a limited range of species of flying insect (typically
70 hymenopterans), relying on naïve males to attempt to mate with the female-mimicking flowers on
71 at least two successive orchid inflorescences (Cozzolino & Widmer, 2005; Jersáková *et al*., 2006;
72 Ayasse *et al*., 2010).
73
74 *Ophrys* flowers use three successive cues to attract insects (Cozzolino & Widmer, 2005;
75 Vereecken *et al*., 2007; Schiestl & Cozzolino, 2008; Schlüter & Schiestl, 2008), each emphasising
76 the labellum. First to impact upon the insect's senses is the complex cocktail of volatile pseudo-
77 pheromones (Borg-Karlson, 1990; Schiestl *et al*., 2003; Mant *et al*., 2005; Vereecken & Schiestl,
78 2009). Next come the visual cues of the flower; initially focusing on the various shapes and
79 colours of the perianth segments in aggregate, the visual focus switches to the labellum as the
80 insect approaches the flower. Once the insect has landed on the labellum, the shape and
81 micromorphological textures of the adaxial epidermis maintain the illusion of a female insect by
82 providing tactile cues that increase the ardour of the male insect and encourage the vertical
83 orientation needed for successful acquisition or deposition of the pollinaria (Kullenberg, 1961).
84
85 Thus far, the olfactory cues of *Ophrys* have received more scientific attention than the visual and
86 tactile cues. Yet the functional morphology of the later-stage cues is equally remarkable; we
87 presume that these contrasting cues are mutually reinforcing (Giurfa *et al*., 1994; Kulachi *et al.*,
88 2008). Many insects use multiple cues to reinforce their search image of a flower, enhancing
89 recognition of target flowers and thus optimizing their foraging efficiency (Whitney *et al*., 2009a;
90 Leonard *et al*., 2011).
91

92 The present study focuses on the impressive visual cues provided by the *Ophrys* labellum, paying
93 particular attention to the speculum, which is a comparatively reflective blue region, varying in
94 complexity of outline, located at or near the centre of the labellum of most *Ophrys* species (Fig.
95 1A). In many species this remarkable feature is generally accepted as mimicking the glossy wings
96 and/or body of the pollinating species, and thus plays a key role in pollination within the genus.
97
98 We selected for study the widespread Mediterranean Mirror Orchid, *Ophrys speculum*, because
99 (as its name suggests) its remarkable speculum is exceptionally large, simple in outline and highly
100 reflective, being perceived by the human eye as a brilliant blue (Fig. 1B). The flower of *Ophrys*
101 *speculum* is known to contain several anthocyanin pigments (Strack *et al.*, 1989), but many
102 authors (including Bradshaw *et al.*, 2010) have speculated that the labellum may owe its
103 remarkable lustre more to physically-induced structural colour than to biochemically induced
104 pigmentation colour.
105
106 Structural components of colour
107 Table 1 provides a series of definitions for optics-based terms used throughout this
108 manuscript. “Colour” is the appearance resulting from the relative amount of light of each
109 wavelength across the human visible wavelength range emanating from an object. This
110 definition can be adapted to take into account the visual capabilities of different animals.
111 Structural colour is the term given to an apparent colour produced by periodically arranged
112 materials that do not necessarily contain pigment. If the scale in which the periodicity occurs
113 is of the same order of magnitude as that of the wavelengths of light striking the object in
114 question, light reflected from the interfaces between the materials interferes constructively for
115 certain wavelengths. This results in reflection and/or transmission of light of different

116 wavelengths in different directions (Kinoshita, 2008). Although several structural mechanisms
117 can generate different colour effects, a defining feature of structural colour is that it is
118 iridescent, or angle dependent – the colour changes as the angle of observation is altered.
119 Pigment-based colours never show this property. However, a structural component can also
120 optically modify a pigment-based colour: in such a case, the appearance of the colour is not
121 only determined by pigments, but also depends on the anatomy of the surrounding structures.
122 For example, the highly reflective yellow colour of the buttercup, *Ranunculus acris*, is caused
123 by structural enhancement of a yellow pigment (Galsterer *et al.*, 1999; Vignolini *et al.*, 2012).
124
125 Structural colour has been well-studied in animals, but its presence in the plant kingdom has
126 only recently begun to be analyzed in detail (Glover & Whitney, 2010). Blue-green
127 iridescence in the leaves of tropical understorey plants has been attributed to multilayered
128 structures (Graham *et al.*, 1993; Gould & Lee, 1996). Similarly, a few reports exist of
129 iridescent blue fruits (Lee, 1991; Lee *et al.*, 2000). We recently described the presence of
130 diffraction gratings on the petals of several angiosperm species, confirming that cuticular
131 striations can generate iridescent colours that are superimposed on the underlying pigment
132 colour (Whitney *et al.*, 2009b).
133
134 In this interdisciplinary study, we apply several analytical techniques with the aim of determining
135 both the causes and relative importance of biochemical and structural effects in producing the
136 much-discussed *Ophrys* 'mirror'. We conclude that the visual effect is the product of a
137 combination of factors. The colour is the product of pigmentation, but the final appearance of the
138 labellum is modified considerably by the combination of this pigment with specular reflection
139 arising from the ultrastructure of the cell wall and cuticle. The labellum does not exhibit *bona fide*

140 iridescence, but its colour does appear angle-dependent as a result of the strong reflection of white
141 light from the glossy cuticle at certain angles.
142
143 **Materials and Methods**
144 Plant material
145 Several plants of *Ophrys speculum* Link were provided by one of us (SM) from his personal
146 collection. Plants in the early stages of flowering were shipped to the Department of Plant
147 Sciences, University of Cambridge, and maintained on a south-facing windowsill with light
148 watering until all flowers had been exploited.
149
150 Optical analysis
151 To determine the colour response of the flower, images were obtained with a standard digital
152 camera and compared with images obtained using a UV-sensitive camera (Fuji Finepix
153 camera equipped with a quartz objective and a Baader U-filter 2" HWB 325-369).
154
155 Reflection measurements were taken from the central blue region of the labellum (speculum)
156 using a commercial reflection/backscattering probe [Ocean Optics]. One end of the probe was
157 directly coupled onto a spectrometer [QE65000 Ocean Optics, 200–950 nm] while the other
158 end was linked to a light source [DH-2000 Deuterium Tungsten Halogen Light Sources]
159 providing illumination with a fixed numerical aperture of 0.22.
160
161 In order to better characterize the optical response of the flower, angular resolved spectra were
162 collected using a goniometer. The illumination arm can be held in a determined fixed position
163 while the sample and the collection arm are rotated independently.

Microscopy

For scanning electron microscope (SEM) examination (Fig. 1C, D), flowers were fixed in formalin acetic alcohol (FAA) and stored in 70% ethanol. Specimens were passed through an ethanol series up to 100% ethanol and critical-point dried using a Tousimis Autosamdri 815B. Specimens were then mounted on aluminium stubs, coated in platinum using a sputter coater (Emitech K550), and examined under a Hitachi S-4700 SEM at 2 kV.

For transmission electron microscope (TEM) examination (Fig. 1E, F), 2 mm squares were dissected from the labellum using a mounted needle, fixed in 2.5% glutaraldehyde in phosphate buffer at pH 7.4, and stored in 70% ethanol until needed. Samples were then stained in 2% osmium tetroxide solution and passed through an ethanol and resin series before being polymerized for 18 h under vacuum. Semi-thin sections (0.5–2 μm) and ultra-thin sections (14 nm) were cut using an ultramicrotome (Reichert-Jung Ultracut). The semi-thin sections were mounted on glass slides and stained with toluidine blue in phosphate buffer, before being examined under a light microscope. The ultra-thin sections were placed on Formvar-coated grids and stained automatically with uranyl acetate and lead citrate using an Ultrastainer (Leica EM Stain) before being examined under the TEM.

For light microscope (LM) examination (Fig. 1G–I), fresh, unstained labella were hand-sectioned using a single-edged razor blade and mounted in a drop of water on a microscope slide, covered with a glass cover slip, and imaged using a Leitz Diaplan photomicroscope fitted with a Leica DC500 digital camera.

188 Metabolite analysis

189 Labella of *Ophrys speculum* were excised from flowers using a razor blade. The inner blue
190 section and the outer brown section were separated under a dissecting microscope, flash-
191 frozen in liquid nitrogen and placed in tubes containing 1 mL cold methanol containing 1%
192 hydrichloric acid. Pigments were extracted by shaking gently overnight at room temperature in
193 the dark and subsequently stored at -80ºC.

194 Absorbance spectra of the crude extracts containing pigments from either the blue or brown
195 regions of the labellum were obtained between 300 and 700 nm on a Jasco V-550 UV-VIS
196 spectrophotometer (Jasco, Essex, UK). As per Davey *et al*. (2004), flavonoids from the crude
197 methanolic extracts were analyzed by High Performance Liquid Chromatography
198 (HPLC:Surveyor system, Thermo Scientific), the eluant being analyzed by both photodiode
199 array (PDA) spectrometry and time-of-flight mass spectrometry using electrospray ionization
200 (Finnigan LCQ DECA XP, Thermo Scientific). Data were analyzed using Xcalibur software
201 (Thermo Fisher Scientific). Samples (injection volume, 20 μL) were resolved on a Luna C18
202 column (250 × 2.0 mm: Phenomenex, UK) using 0.5% formic acid (solvent A) and acetonitrile
203 (solvent B); with a gradient of increasing B such that initial A:B (95:5 v/v); 2 min (95:5); 42
204 min (0:100); 47 min (0:100); 48 min (95:5); 53 min (95:5), at a flow rate of 0.2 mL min^{-1}. The
205 eluant was monitored for absorbance between 200 and 800 nm with the MS operating in
206 positive ion mode (settings: capillary temperature 230ºC; capillary voltage 27 V; spray voltage
207 3.5 kV; sheath gas flow rate 9.28 (arb.)); centroid data collection). Mass ions were detected
208 between 100 and 1200 *m/z*, using quercetin (Sigma) to tune and calibrate the MS. Metabolite
209 fragmentation (ms/ms) on selected masses was carried out under the following settings:
210 isolation width 1.0 *m/z*, 50% normalized collision energy, activation Q = 0.250, activation

211 time 30 msec. The identification of metabolites was based on their absorbance spectra and
212 mass spectral data as compared with published data (the online flavonoid database at
213 http://metabolomics.jp/wiki/Index:FL) and with a reference flavonol, quercetin-3-β-D-
214 glucoside, 20 μM and anthocyanin, cyanidin 3-O-glucoside chloride, 200μM (Sigma).

215

216 **Results**

217 The speculum has a smooth, flat surface with disordered layers in the cell wall

218 The labellum of *Ophrys speculum* (Fig. 1A, B) has a complex adaxial epidermal surface (see
219 also Bradshaw *et al.*, 2010). Its epidermal cells are either smooth, non-striated and non-
220 papillate, or consist of long, spirally twisted trichomes, the latter concentrated along the
221 periphery of the labellum (Fig. 1C).

222

223 The adaxial epidermis of the speculum region is composed entirely of smooth, flat-topped
224 cells (Fig. 1D) that show little or no doming in transverse section (Fig. 1E, G). Each epidermal
225 cell contains a large vacuole, most of the cytoplasm and organelles lying close to the inner cell
226 wall (Fig. 1E). The epidermis of the speculum incorporates the bulk of the blue pigment (Fig.
227 1G, I), as does the epidermis of heavily pigmented regions located elsewhere in the flower.
228 When the fresh tissue of the speculum is cut the blue colour leaches out rapidly (Fig. 1H). The
229 epidermal cell wall is thickest on the outer surface, where it is overlain by a thick (*ca* 0.5 μm)
230 cuticle that covers the entire surface. Although the cutinized cell wall displays some layering
231 (Fig. 1F), our TEM images do not indicate an ordered multilayered structure of sufficient
232 regularity and dimensions to generate structural colour of the kind responsible for the blue
233 scales of *Morpho* butterfly wings (Vukusic *et al*., 1999).

234

The speculum is highly UV-reflective

Although the blue colour of the speculum is exceptionally striking to the human eye, many insects perceive colours differently from human vision. In particular, it is common for insects to perceive light in the ultraviolet range of the spectrum (Briscoe & Chittka, 2001). To assess whether the *Ophrys* labellum is UV reflective, we compared a photograph of the flower taken using a standard camera with one taken with maximal sensitivity in the 325–369 nm range (Fig. 2A, B). It is clear from these images that the blue speculum region of the labellum is highly UV reflective. The reflectivity in this range has two components – it is due partly to the specular reflected signal from the cuticle and partly to a more diffuse signal caused by light that has entered the cells but not been absorbed by the pigment within.

To investigate this response more fully we compared the reflection of the labellum of mature and senescent flowers using a commercial reflection/backscattering probe [Ocean Optics]. A peak of reflection was observed between 350 and 400 nm (Fig. 2C) in both flowers but was more evident in the mature flower, confirming that a strong UV signal is detectable from the labellum of a receptive flower. This UV signal is likely to enhance the salience of the speculum, potentially facilitating pollinator landing on the labellum.

The speculum reflects white light strongly in the specular direction but blue light at other angles

In order to better characterize the optical response of the speculum, angular resolved spectra were collected using a goniometer (a schematic diagram of the experimental setup is presented in Fig. 3A). Figure 3B shows the scattering behaviour of the speculum in colour scale blue to green to yellow (the yellow colour in the chart shows a greater proportion of reflected light

compared to blue). The collection angle is plotted on the Y axis and the wavelength on the X axis. At the specular reflection direction (indicated by the white dotted line in the image) the absorption from the pigment is less significant compared with the other scattering angles. Specular reflection is reflection of white light at the same angle as it arrives at a surface, as seen most strongly in a mirror. Across the horizontal band between 20 and 40°, light of all wavelengths is reflected equally across the spectrum, constituting an angularly broadened mirror-like response. This behaviour is in contrast with a perfectly planar surface where specular reflection occurs only for a collection angle of 30° matching the illumination angle. However, since the reflective surface of the speculum is convex and the diameter of the illumination spot on the sample is ~2 mm, the light is reflected not only at one specific angle but in the angular range between 20° and 40°.

Above ~40° light reflection is limited predominantly to the UV-blue and the infrared. This analysis suggests that the speculum contains a pigment that absorbs in the wavelength window between 420 and 650 nm. The combination of such a pigment with the specular reflection from a mirror-like surface results in a speculum that appears blue at high observation angles but whiter in a specular observation direction.

The contribution of specular reflection to the total reflectivity of the speculum is analyzed further in Fig. 3C, where the integrated intensity as a function of the collection angle is recorded for two contrasting incidence angles (15° and 60°) and two wavelength regions. In the polar graph the integrated intensity is shown for the two incidence angles of 15° (solid lines) and 60° (dashed lines) and for the two wavelength regions of 300-400 nm, where the pigment does not absorb (red), and 500-600 nm, where the pigment does absorb (black). For

an angle of incidence of 15°, glossiness is dominant and the light is almost entirely reflected in the specular reflection direction across the entire spectrum. This result suggests that the optical appearance of the speculum results from the interplay of the glossy cuticle and the diffuse blue and UV light filtered by the pigment. At low illumination and observation angles the signal from the air–cuticle interface predominates, resulting in a broad-band (white) gloss. At larger angles of incidence (dashed lines), the contribution of the specular reflection is much smaller, making the spectral response of pigment scattering across a wide angular range more clearly visible. This observation is explained by blue (and UV) diffuse isotropic scattering from the pigment–bearing tissue and specular reflection arising from the smooth surface. Finally, the red dashed line spans a greater angular range than the black dashed line, presumably because the pigment within the tissue absorbs some light in the 300–400 nm range.

<u>The speculum contains only cyanidin pigments, whereas the rest of the labellum also contains delphinidin and quercetin</u>

Absorption spectra of the crude extracts were obtained from the blue speculum, brown labellum fringe and the yellow lateral petals (Fig. 4). Peak absorption in the 500–560 nm regions indicated the presence of anthocyanins with λ_{max} at *ca* 529 nm (Harborne, 1984: 64–65). Absorption between 350 and 380 nm in the brown labellar margin suggested the possible presence of flavonols acting as co-pigments (Shoji *et al*., 2007). Absorption peaks at 419 nm and 653 nm indicated the presence of chlorophyll *a*, especially in the yellow lateral petals.

The speculum

Only one pigment from the blue speculum was resolved at 17.97 min by HPLC (Figs. 5, 6). The absorption spectrum and the λ_{max} of 516 nm and 280 nm of the metabolite at this time

307 indicated a structure resembling anthocyanins. This spectrum matched published spectra of
308 cyanidin-3-glucoside or cyanidin-3-sophoroside (Zhang *et al*., 2008), malonyl ester of
309 cyanidin-3-glucoside (Lee, 2002) and cyanidin-3-glucoside or peonidin-3-glucoside (Hong &
310 Wrolstad, 1990). The molecular mass ions of the metabolite eluting at 17.97 min were
311 determined in the positive ionization mode. The total mass scan of the peak detected the
312 molecular mass ions *m/z* 535, 593, 611 and 758 (Table 2). These masses were searched against
313 the online flavonoid database at http://metabolomics.jp/wiki/Index:FL and in published
314 manuscripts. The parent anthocyanin aglycone proved to be a cyanidin (Giusti *et al.* 1999a, b;
315 Zhang *et al*., 2008; Mullen *et al*., 2010) with the following putative identifications for *m/z*: 535
316 cyanidin 3-(3"-malonylglucoside), 593 cyanidin 3-(6"-dioxalylglucoside), 611 cyanin or
317 cyanidin 3,5-diglucoside and 758 gentiocyanin C or cyanidin 3-glucoside-5-(6-p-
318 coumaroylglucoside). Fragmentation spectra were obtained for the parent mass ion of 534,
319 which produced daughter ions of 448.9 and 287.04 *m/z*. According to Giusti *et al*. (1999a, b)
320 and Mullen *et al*. (2010), the mass 535.3 is the cyanidin 3-(3-malonylglucoside), which is the
321 mass of cyanidin (287) + hexose minus H_2O (162.2) + malonic acid minus H_2O (86.1). When
322 cyanidin 3-(3-malonylglucoside) is fragmented it also produces the mass 449.1 (535-86.1),
323 corresponding with cyanidin 3-(3-malonylglucoside) minus the malonyl group. The mass ion
324 287 is also produced by cyanidin 3-(3-malonylglucoside) (449.1) minus the mass of hexose
325 (162.2), thus forming the cyanidin aglycone. It was not possible to obtain an authentic
326 standard for cyanidin 3-(3-malonylglucoside); instead cyanidin 3-O-glucoside chloride was
327 used to confirm the absorption spectrum (λ_{max} of 514 nm and 280 nm), parent mass (449.01,
328 minus chloride ion) and fragmentation pattern (forms the mass of cyanidin (287) minus the
329 glucoside) of a cyanidin-glycoside (Table 2, Fig. 6H).
330

331 *Brown labellum fringe*

332 Six peaks were resolved in the brown section chromatogram (Figs. 5, 6). The absorption
333 spectra of two peaks (retention times 17.9 and 18.6 min) were characteristic of an anthocyanin
334 and four peaks (retention times 18.4, 19.3, 20.3 and 21.1 min) were characteristic of flavonols
335 (Mabry *et al*., 1970). The peak eluting at 17.92 min had the same absorption spectrum, parent
336 ion and fragment ion mass as that found at a similar time in the blue section, and hence was
337 identified as cyanidin 3-(3"-malonylglucoside). The peak at retention time 18.6 min, slightly
338 co-eluted with another peak at 18.4 min and had a λ_{max} of 522 nm, indicating the presence of
339 delphinidin-3-rutiniside or cyanidin-3-rutiniside (Toki *et al*., 1996; Vera de Rosso &
340 Mercadante, 2007). The remaining peaks at 18.4, 19.3, 20.3 and 21.1 min all had absorption
341 spectra with a λ_{max} of 356 nm that are characteristic of a flavonol such as isorhamnetin-
342 rutinoside (λ_{max} 356 nm) or a glycoside of quercetin such as quercetin-glucoside, -rutinoside or
343 -rhamnoside (λ_{max} 358 nm) (Mabry *et al*., 1970). The mass spectra of these four flavonol peaks
344 all revealed mass ions of the same molecular weight as glycosylated or malonylated quercetin
345 (Table 2). Variation in the conjugate species explains the differences in retention time for the
346 same quercetin compound. The masses of other compounds, especially the flavonols luteolin
347 and kaempferol, were also present in the online mass searches. However, the *Ophrys* labellum
348 compound is unlikely to have these chemistries, as the UV traces for these compounds are
349 closer to 330 nm and 370 nm, respectively. The reference compound quercetin-3-β-D-
350 glucoside had a similar retention time to the four flavonols in the extract and had a λ_{max} of 356
351 nm. Therefore, the main compound present in the labellar fringe is likely to be a mix of
352 cyanidin and delphinidin with a co-pigment of quercetin.
353

354 **Discussion**

355 Analysis of the optical properties of the intensely blue-coloured speculum of *Ophrys speculum*
356 indicates that the visual effects are achieved by multiple factors. A pigment located in the
357 adaxial epidermis, absorbing in the green–red region of the spectrum and diffusely reflecting
358 blue and UV light, operates in combination with a highly reflective mirror-like surface that
359 provides intense specular reflection and causes the blue colour to be somewhat angle-
360 dependent. UV photography and simple reflectance spectrometry indicate that the speculum is
361 highly reflective in the UV, a part of the spectrum known to be visible to many insects,
362 including the hymenopteran pollinators characteristic of *Ophrys* flowers (Briscoe & Chittka,
363 2001). The high degree of salience (conspicuousness) that this UV signal provides to the
364 *Ophrys speculum* flower is likely to enhance pollinator handling of the flower, perhaps
365 facilitating landing in the optimal position for pseudo-copulation and eventual pollen transfer.
366
367 The intense specular reflection from the labellum provides the characteristically extreme
368 glossiness, a feature that has been hypothesized to improve the sexual mimicry of the flower
369 by resembling the sheen on the folded wings of an insect at rest. A similar glossiness has been
370 reported for some other flowers. For example, the dark petal spots of *Gorteria diffusa*, a South
371 African daisy, achieves pollination by mimicking female bombyliid flies; here too, glossiness
372 has been hypothesized to mimic the visual appearance of folded insect wings (Ellis &
373 Johnson, 2010). Our micrographs indicate that the glossiness arises from a thick (*ca* 0.5 μm)
374 and extremely smooth, ridgeless layer of cuticle deposited on top of unusually flat epidermal
375 cells. The cuticle layer extends between cells, reducing the visibility of individual cell
376 boundaries. The overall effect produced by this cuticular layer is of a thin mirror coating the
377 flower surface. The highly reflective yellow colour of the buttercup, *Ranunculus acris*, is also

the result of a mirror-like cuticle (Galsterer *et al.*, 1999; Vignolini *et al.*, 2012). The *Ophrys speculum* mirror layer is made more effective by the flatness of the adaxial epidermal cells. Petal epidermal cells are frequently conical-papillate (Kay *et al.*, 1999; Whitney *et al.*, 2011) and failing that, they are usually lenticular or gently domed. The extreme flatness of the epidermal cells in the speculum region provides a better backdrop to the mirror than a biological surface can usually achieve.

Analysis of the reflection of different wavelengths of light from the speculum at different angles confirms that there is a structural component to the appearance of the speculum. At the specular angle (set at 30° in our analysis) light of all wavelengths is reflected with equal efficiency. Similar results are obtained with different angles of incidence. However, at increased angles of collection relative to the sample a strong blue and UV reflection is observed; little if any reflection of other wavelengths is evident until the far-red region of the spectrum is reached. This analysis explains why the colour of the speculum appears to shift as the flower is re-oriented. At angles where the specular reflection is strong, a mirror-like effect dilutes the apparent blueness of the tissue. However, when the flower is shifted to angles other than the specular, the intense blue reflection again dominates the signal. In addition, the gently convex shape conferred on the speculum by curvature of the labellum contributes to the apparent shift of colour with angle of observation, by modifying the contribution of the gloss. These effects are evident in Fig. 1B, where some apparent blue and white speckling observed under strong specular illumination is the result of slight variations in angle and cuticle thickness across the surface of the speculum. This angular dependence is a defining feature of a structural contribution to colour, but in this case there is no evidence that the blue hue itself is produced through structural means. If the blue colour was achieved by a multi-layered

structure, as is the case for the *Morpho* butterfly, the hue of the colour (that is, the relative amounts of blue, green, yellow and/or red light) would change at different observation angles (Vukusic *et al.*, 1999). Instead, it is only the relative contributions of blue and broad-band reflected (white) light, not blue and other narrow bandwidths of light, that alter as angle varies. Accordingly we cannot define the speculum as truly iridescent. In response to the description by Bradshaw *et al.* (2010) of epidermal morphology of the labellum of a range of *Ophrys* species, Vereecken *et al.* (2011) also reported that unpublished data suggested that the *Ophrys speculum* labellum was not truly iridescent. In further support of this observation we note that, although the cell walls of the speculum epidermal cells appear to contain layers of cellulose in our TEM analysis, those layers are irregular in depth and shape. Only regular structures can generate colour by interference, whereas the disordered layering evident in Fig. 1F is unable to generate a colour signal.

Our optical analysis indicated the likely presence of a blue pigment in the speculum, absorbing light between 420 and 650 nm. Biochemical analysis confirmed the presence of an anthocyanin, cyanidin 3-(3"-malonylglucoside). This was the only pigment detected in the speculum tissue, using an analytical approach competent to reveal any flavonoids present. Anthocyanins are commonly found in flowers, generating the red–blue range of colours. Cyanidins produce a bluer colour than some other anthocyanins, such as pelargonidins, although they are usually more magenta than purple/blue. The particular hue produced by the cyanidin is determined by several other factors, including the nature of any side groups on the molecule, their interactions with metal ions, the pH of the vacuolar liquid and the co-occurrence of any other pigments. It is likely that an alkaline vacuolar pH or formation of a complex with iron or magnesium ions is responsible for the blue hue of this cyanidin, although

426 further analyses of cellular ion content would be necessary to define how the particular shade
427 is produced. Although we detected chlorophyll in the biochemical analysis, it was primarily
428 found in the brown fringes of the labellum, so it is unlikely that this pigment is contributing
429 greatly to the blue colour of the speculum. George *et al.* (1973) also found cyanidins in the
430 intense blue-purple flowers of the Australian enamel orchids (*Elythranthera* spp.) from
431 Australia, though it remains to be determined whether there is a structural component to the
432 appearance of these highly glossy flowers.
433
434 We detected the presence of the same cyanidin and possibly also delphinidin-3-rutiniside in
435 the region of the labellum surrounding the speculum. This tissue also contains four co-
436 pigments of a flavonol, which are most likely glycosylated or malonylated quercetins. The
437 flavonols appear to modify the absorption range of the anthocyanins to produce a brown
438 colouration in the tissue. It is the exclusion of the flavonoid co-pigments from the speculum
439 that permits the striking purity of the blue colour of the cyanidin in the labellum of *Ophrys*
440 *speculum*.
441
442 The pure glossy blue of the *Ophrys speculum* flower has fascinated scientists and naturalists
443 for many years. The intensity of the colour, and its apparent angular dependence, led to
444 speculation that it is produced using structural rather than pigment-based mechanisms (cf.
445 Bradshaw *et al*., 2010). From our analysis, we conclude that the visual effect is the product of
446 a combination of factors – the colour is the result of pigmentation, but the final appearance of
447 the labellum is modified by the combination of this pigment with the specular reflection
448 arising from the ultrastructure of the cell wall and cuticle. A single pure cyanidin produces the
449 basic blue colour, most likely as a result of an alkaline vacuolar pH or formation of a complex

with metal ions. The spectral purity of the pigment colour is enhanced by backscattering from a disordered multilayer structure in the lower wall of the epidermal cells. The flat surface of the epidermal cells is enhanced by an exceptionally smooth mirror composed of cuticle, providing both glossiness and a strong specular reflection, which is angle dependent even though the colour itself is not iridescent. In combination, these features produce a striking optical effect that presumably contributes to the pollination efficiency and thus potentially to the reproductive success of the species.

Acknowledgements

We thank Matthew Dorling for excellent plant care and Jeremy Baumberg for helpful discussions. This work was funded by a CoSyst grant provided by the UK Biotechnology and Biological Sciences Research Council and administered by the Systematics Association and the Linnean Society (PIs Glover & Bateman) and by a grant from the Leverhulme Trust (PI Glover: F/09-741/G).

References

Ayasse M, Gögler J, Stökl J. 2010. Pollinator-driven speciation in sexually deceptive orchids of the genus *Ophrys.* In M Glaubrecht (editor), *Evolution in action.* Berlin: Springer, 101–118.

Borg-Karlson A. 1990. Chemical and ethological studies of pollination in the genus *Ophrys* (Orchidaceae). *Phytochemistry* **29:** 1359–1387.

Bradshaw E, Rudall PJ, Devey DS, Thomas MM, Glover BJ, Bateman RM. 2010. Comparative labellum micromorphology of the sexually deceptive temperate orchid genus *Ophrys*: diverse epidermal cell types and multiple origins of structural colour. *Botanical Journal of the Linnean Society* **162:** 504–540.

Briscoe AD, Chittka L. 2001. The evolution of color vision in insects. *Annual Review of Entomology* **46:** 471–510.

Cozzolino S, Widmer A. 2005. Orchid diversity: an evolutionary consequence of deception? *Trends in Ecology and Evolution* **20:** 487–494.

Darwin C. 1862. *The various contrivances by which British and foreign orchids are fertilised by insects.* London: A & C Black.

Davey MP, Bryant DN, Cummins I, Gates P, Ashenden TW, Baxter R, Edwards R. 2004. Effects of elevated CO_2 on the vasculature and phenolic secondary metabolism of *Plantago maritima. Phytochemistry* **65:** 2197–2204.

Ellis AG, **Johnson SD. 2010.** Floral mimicry enhances pollen export: the evolution of pollination by sexual deceit outside of the Orchidaceae. *American Naturalist* **176:** E143–E151.

Galsterer S, Musso M, Asenbaum A, Furnkranz D. 1999. Reflectance measurements of glossy petals of *Ranunculus lingua* (Ranunculaceae) and of non-glossy petals of *Heliopsis helianthoides* (Asteraceae). *Plant Biology* **1:** 670–678.

George A, Gonzales C, Strauss MS, Arditti J. 1973. Chemotaxonomic and ecological implications of anthocyanins in *Elythranthera. Biochemical Systematics* **1**: 45–49.

Giurfa M, Núñez, J, Backhaus W. 1994. Odour and colour information in the foraging choice behavior of the honeybee. *Journal of Comparative Physiology A* **175:** 773–779.

Giusti MM, Rodríguez-Saona LE, Griffin D, Wrolstad RE. 1999a. Electrospray and tandem mass spectroscopy as tools for anthocyanin characterization. *Journal of Agriculture and Food Chemistry* **47:** 4657–4664.

Giusti MM, Rodríguez-Saona LE, Wrolstad RE. 1999b. Molar absorptivity and color characteristics of acylated and non-acylated pelargonidin-based anthocyanins. *Journal of Agriculture and Food Chemistry* **47:** 4631–4637.

498 **Glover BJ, Whitney H. 2010.** Iridescence and structural colour in plants – the poorly studied
499 relatives of pigment colour. *Annals of Botany* **105:** 505–511.
500 **Gould KS, Lee DW. 1996.** Physical and ultrastructural basis of blue leaf iridescence in four
501 Malaysian understory plants. *American Journal of Botany* **83:** 45–50.
502 **Graham RM, Lee DW, Norstog K. 1993.** Physical and ultrastructural basis of blue
503 iridescence in two neotropical ferns. *American Journal of Botany* **80:** 198–203.
504 **Harborne JB. 1984.** *Phytochemical methods – a guide to modern techniques of plant analysis*
505 (2nd edition). London: Chapman & Hall.
506 **Hong V, Wrolstad RE. 1990.** Use of HPLC separation/Photodiode Array Detection for
507 characterization of anthocyanins. *Journal of Agriculture and Food Chemistry* **38:** 708–715.
508 **Jersáková J, Johnson SD, Kindlmann P. 2006.** Mechanisms and evolution of deceptive
509 pollination in orchids. *Biological Reviews* **81:** 213–235.
510 **Kay QON, Daoud HS, Stirton CH. 1981.** Pigment distribution, light reflection and cell
511 structure in petals. *Botanical Journal of the Linnean Society* **83:** 57–84.
512 **Kinoshita S. 2008.** Structural colors in the realm of nature, World Scientific Publishing Co.
513 Singapore.
514 **Kulachi IG, Dornhaus A, Papaj DR. 2008.** Multimodal signals enhance decision making
515 in foraging bumblebees. *Proceedings of the Royal Society of London B* **275:** 797–802.
516 **Kullenberg B. 1961.** Studies in *Ophrys* pollination. Zoologiska Bidrag från
517 Uppsala **34**: 1–340.
518 **Lee DW. 1991.** Ultrastructural basis and function of iridescent blue colour of fruits in
519 *Elaeocarpus*. *Nature* **349:** 260–262.
520 **Lee DW, Taylor GT, Irvine AK. 2000.** Structural fruit coloration in *Delarbrea michieana*
521 (Araliaceae). *International Journal of Plant Science* **161:** 297–300.

Lee HS. 2002. Characterization of major anthocyanins and the color of red-fleshed Budd Blood Orange (*Citrus sinensis*). *Journal of Agriculture and Food Chemistry* **50:** 1243–1246.

Leonard AS, Dornhaus A, Papaj DR. 2011. Flowers help bees cope with uncertainty: signal detection and the function of floral complexity. *Journal of Experimental Biology* **214:** 113–121.

Mabry TJ, Markham KR, Thomas MB. 1970. *The systematic identification of flavonoids.* New York: Springer-Verlag..

Mant J, Peakall R, Schiestl FP. 2005. Does selection on floral odor promote differentiation among populations and species of the sexually deceptive orchid genus *Ophrys*? *Evolution* **59:** 1449–1463.

Mullen W, Larcombe S, Arnold K, Welchman H, Crozier A. 2010. Use of accurate mass full scan mass spectrometry for the analysis of anthocyanins in berries and berry-fed tissues. *Journal of Agriculture and Food Chemistry* **58:** 3910–3915.

Rudall PJ, Bateman RM. 2002. Roles of synorganisation, zygomorphy and heterotopy in floral evolution: the gynostemium and labellum of orchids and other lilioid monocots. *Biological Reviews* **77:** 403–441.

Schiestl FP, Cozzolino S. 2008. Evolution of sexual mimicry in the orchid subtribe Orchidinae: the role of preadaptations in the attraction of male bees as pollinators. *BMC Evolutionary Biology* **8:** 27 [10 pp.].

Schiestl FP, Peakall R, Mant JG, Ibarra F, Schulz C, Franke S, Franke W. 2003. The chemistry of sexual deception in an orchid–wasp pollination system. *Science* **302:** 437–438.

Schlüter PM, Schiestl FP. 2008. Molecular mechanisms of floral mimicry in orchids. *Trends in Plant Science* **13:** 228–235.

Shoji K, Miki N, Nakajima N, Momonoi K, Kato C, Yoshida K. 2007. Perianth bottom-specific blue color development in tulip cv. Murasakizuisho requires ferric ions. *Plant and Cell Physiology* **48:** 243–251.

Strack D, Busch E, Klein E. 1989. Anthocyanin patterns in European orchids and their taxonomic and phylogenetic relevance. *Phytochemistry* **28:** 2127–2139.

Toki K, Takeuchi M, Saito N, Honda T. 1996. Two malonylated anthocyanidin glycosides in *Ranunculus asiaticus. Phytochemistry* **42:** 1055–1057.

Vera De Rosso V, Mercadante AZ. 2007. HPLC–PDA–MS/MS of anthocyanins and carotenoids from Dovyalis and Tamarillo fruits. *Journal of Agriculture and Food Chemistry* **55:** 9135–9141.

Vereecken NJ, Mant J, Schiestl FP. 2007. Population differentiation in female mating signals and male preferences in a solitary bee. *Behavioural Ecology and Sociobiology* **61:** 811–821.

Vereecken NJ, Schiestl FP. 2009. On the roles of colour and scent in a specialized floral mimicry system. *Annals of Botany* **104:** 1077–1084.

Vereecken NJ, Streinzer M, Ayasse M, Spaethe J, Paulus H, Stokl J, Cortis P, Schiestl, F. 2011. Integrating past and present studies on *Ophrys* pollination – a comment on Bradshaw *et al. Botanical Journal of the Linnean Society* **165**: 329-335.

Vignolini S, Thomas M, Kolle M, Wenzel T, Rowland A, Rudall PJ, Baumberg JJ, Glover BJ, Steiner U. 2012. Directional scattering from the glossy flower of *Ranunculus*: how the buttercup lights up your chin. *Interface* **9**: 1295-1301.

Vukusic P, Sambles JR, Lawrence CR, Wootton RJ. 1999. Quantified interference and diffraction in single *Morpho* butterfly scales. *Proceedings of the Royal Society B* **266:** 1403–1411.

569 **Whitney HM, Chittka L, Bruce T, Glover BJ. 2009a.** Conical epidermal cells allow bees to
570 grip flowers and increase foraging efficiency. *Current Biology* **19:** 1–6.
571 **Whitney HM, Kolle M, Andrew P, Chittka L, Steiner U, Glover BJ. 2009b.** Floral
572 iridescence, produced by diffractive optics, acts as a cue for animal pollinators. *Science* **323:**
573 130–133.
574 **Whitney HM, Bennett KVM, Dorling MW, Prince D, Sandbach L, Chittka L, Glover BJ.**
575 **2011.** Why do so many petals have conical epidermal cells? *Annals of Botany* **108:** 609–616.
576 **Zhang Y, Liao X, Chen F, Wu J, Hu X. 2008.** Isolation, identification, and color
577 characterization of cyanidin-3-glucoside and cyanidin-3-sophoroside from red raspberry.
578 *European Food Research and Technology Journal* **226:** 395–403.
579
580

581 Table 1: Glossary of terms from the field of optics used within this manuscript

582

Term	*Definition*
Colour	Appearance resulting from the relative amount of light emanating from an object at each wavelength. The perceived colour depends on the receptivity of the photoreceptors in the eye of the observer.
Structural colour	Colour produced by light interference rather than pigmentation. Reflection of particular wavelengths of light by periodically arranged materials causes colour, irrespective of the chemical characteristics of the material (including whether or not it contains pigments).
Iridescence	An optical effect where the apparent colour of an object changes as the angle of observation is altered, as a consequence of different wavelengths of light being reflected at different angles.
Specular reflection	Reflection of white light at the same angle as it arrives at a surface, as seen most strongly in a mirror.
Salience	Conspicuousness against the background – a red button is more salient on a blue coat than a blue button.

583

584 Table 2: High Performance Liquid Chromatography (HPLC) and mass spectrometry (MS)
585 analysis of extract from the blue speculum and brown labellum fringe sections of *Ophrys*
586 *speculum*. HPLC: RT = retention time in minutes; λ_{max} = maximum absorption between 200
587 and 800 nm on the photodiode array detector; MS: main parent monoisotopic mass ions
588 (positive ionization) of each peak and the fragment ions where detected. Metabolite
589 identification was based on reference to published data and by searching the monoisotopic
590 mass ions on the flavonoid database at http://metabolomics.jp/wiki/Index:FL For each mass,
591 more than one metabolite is usually identified on the database, therefore only one example for
592 each mass is provided here.
593

	Peak RT (min)	λ_{max}	Parent ions *m/z*	Fragment ions *m/z*	Putative metabolite identification
Blue	17.97	516, 280	534.90	448.9, 287.04	Cyanidin 3-(3"-malonylglucoside),
			592.78		Cyanidin 3-(6"-dioxalylglucoside),
			611.16		Cyanin or Cyanidin 3,5-diglucoside
			757.86		Cyanidin 3-glucoside-5-(6-p-coumaroylglucoside)
Brown	17.97	515, 280	534.90	448.9, 287.04	Cyanidin 3-(3"-malonylglucoside),
			592.78		Cyanidin 3-(6"-dioxalylglucoside),
			611.16		Cyanin or Cyanidin 3,5-diglucoside
			757.86		Cyanidin 3-glucoside-5-(6-p-coumaroylglucoside)
	18.42	356	534.90	448.9, 287.04	Cyanidin 3-(3"-malonylglucoside),
	18.64	522, 356	460.7		Apigenin 7-(6"-methylglucuronide)
			550.9		Quercetin 3-(6"-malonylgalactoside)
			609.9		Quercetin 3-galactoside-7-rhamnoside
			684.9		Delphinidin 3-(6"-malonylsambubioside)
	19.36	355	609.9		Quercetin 3-glucoside-7-rhamnoside
			685.9		Delphinidin 3-(6"-malonylsambubioside)
			712.7		Quercetin 3-(6"-malonylglucoside)-7-glucoside
			765.05	658.69, 496.83	Myricetin 3-O-(4"-O-acetyl-2"-O-galloyl)-alpha-L-rhamnopyranoside (for 658 fragment)
			804.78		Gossypetin 3-sophoroside-8-glucoside
			927.2	658.93, 496.87	Myricetin 3-O-(4"-O-acetyl-2"-O-galloyl)-alpha-L-rhamnopyranoside (for 658 fragment)
	20.37	356	590.3		Quercetin 3-(2",3",4"-triacetylgalactoside)
			610.49		Quercetin 3-glucoside-7-rhamnoside
			683.96		Delphinidin 3-(6"-malonylsambubioside)
			759.9		Delphinidin 3-sambubioside-5-glucoside
			764.99	658.85, 496.74	Myricetin 3-O-(4"-O-acetyl-2"-O-galloyl)-alpha-L-rhamnopyranoside (for 658)
			927.12	658.97, 552.57	Myricetin 3-O-(4"-O-acetyl-2"-O-galloyl)-alpha-L-rhamnopyranoside (for 658)
			1021		Cyanidin 3-(6-malonylglucoside)-7-(6-caffeoylglucoside)-3'-glucoside
			1181		Cyanidin 3-(6"-p-coumaryl-2'"-sinapylsambubioside)-5-(6-malonylglucoside)
	21.11	356	425.7		Quercetin 7,3',4'-trimethyl ether 3-sulfate
			494.1		Quercetagetin 3'-methyl ether 3-glucoside
			550.7		Quercetin 3-(6"-malonylgalactoside)
			684.83		Delphinidin 3-(6"-malonylsambubioside)
			759.7		Quercetin 3-sambubioside-7-glucoside
Quercetin	20.17	356	464.09	396.08	Quercitin-3-β-D-glucoside

598 **Figure Legends**

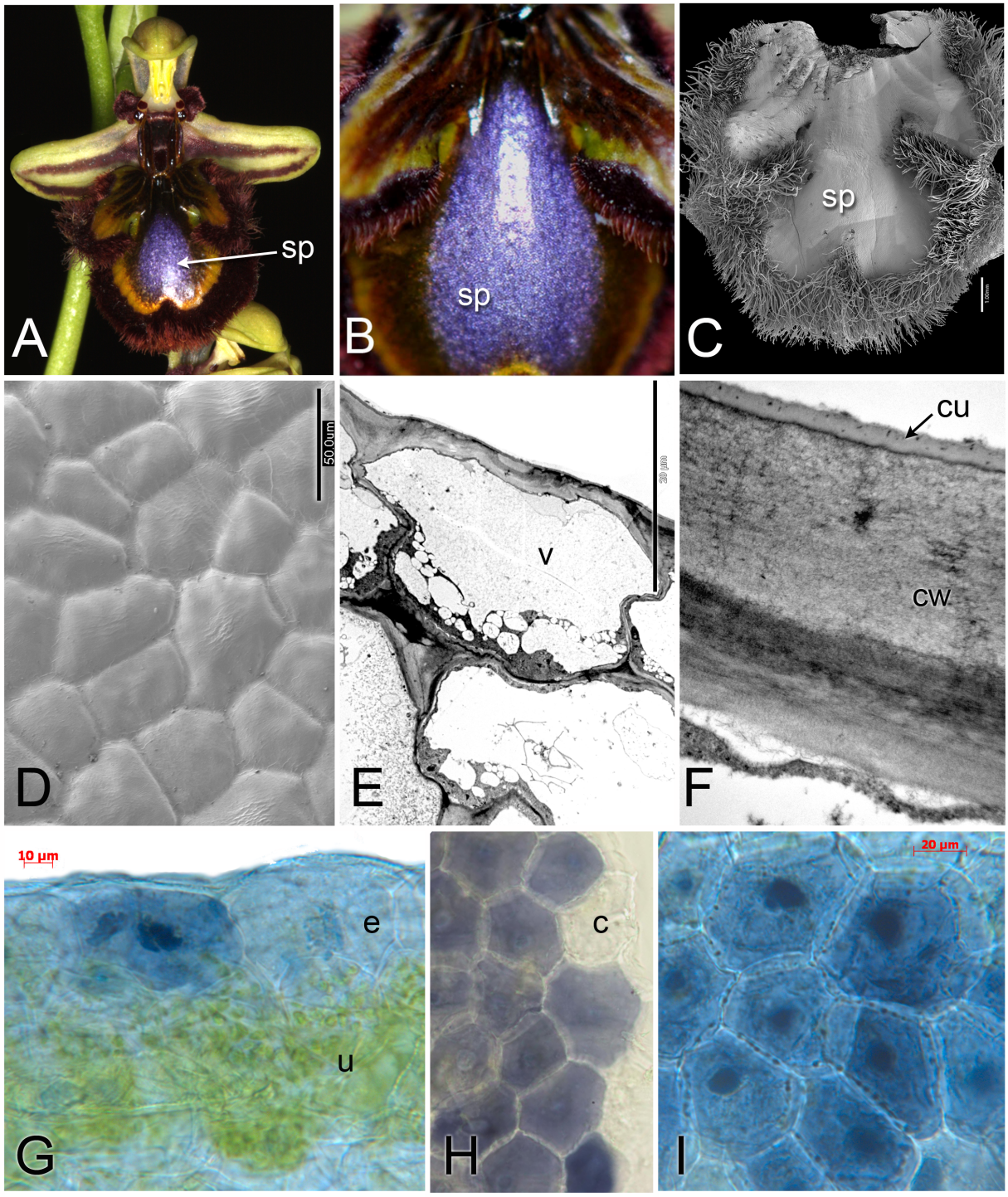

599
600 **Fig. 1** Flower of *Ophrys speculum*; imaged using a standard digital camera (A, B), SEM (C,

601 D), TEM (E, F) and LM of unstained material (G–I). A. Entire flower from above. B. Close-

602 up view of the blue speculum region of the labellum. C. Entire dissected labellum, showing
603 smooth central speculum (sp) and peripheral trichomes. D. Detail of the smooth speculum
604 surface. E. Transverse section of adaxial epidermis of speculum. F. Detail of outer wall (cw)
605 and cuticle (cu) of speculum epidermis. G. Transverse section of unstained dissected
606 speculum, showing adaxial epidermis (e) containing blue pigment and underlying layers
607 containing green chloroplasts. H, I. Surface views of blue adaxial epidermis; blue colour has
608 leached out of cut epidermal cells in (H). Key: c = cut cell, cu = cuticle, cw = cutinized cell
609 wall, e = adaxial epidermis, p = pigment, sp = speculum, v = vacuole.

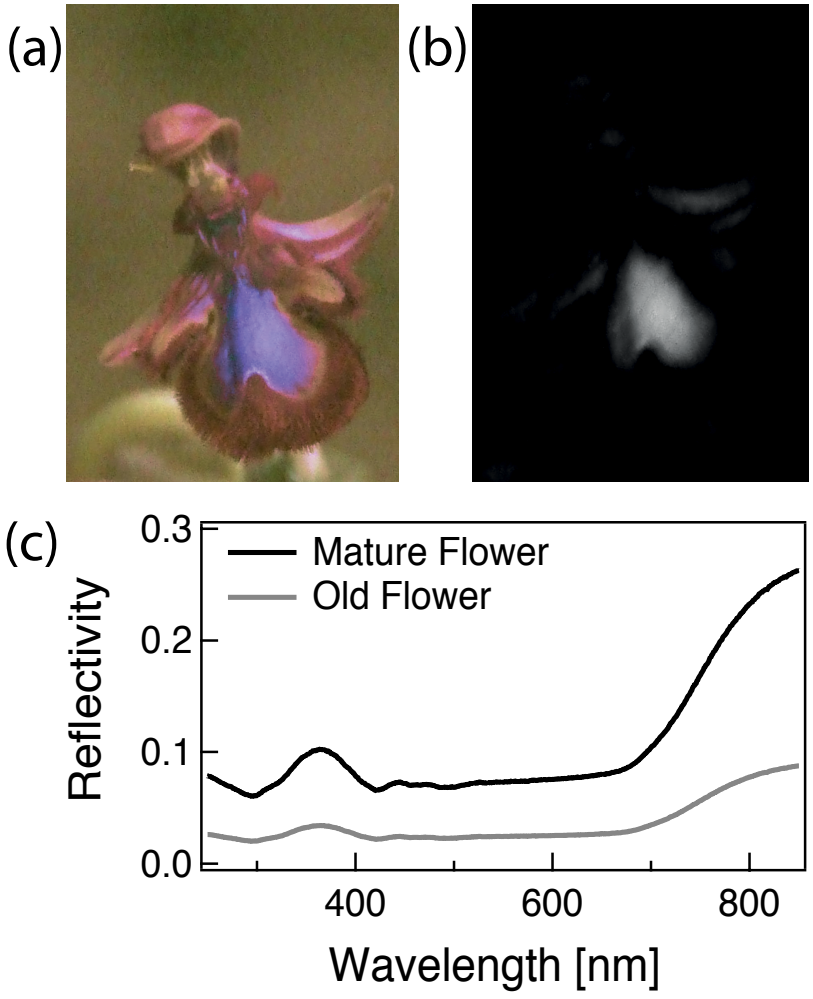

610

611 **Fig. 2** Reflectance from the *Ophrys speculum* flower. A. Flower photographed under daylight.
612 B. The same flower photographed with a UV-sensitive camera. C. Reflectance spectra of
613 mature (black line) and senescent (grey line) flowers.

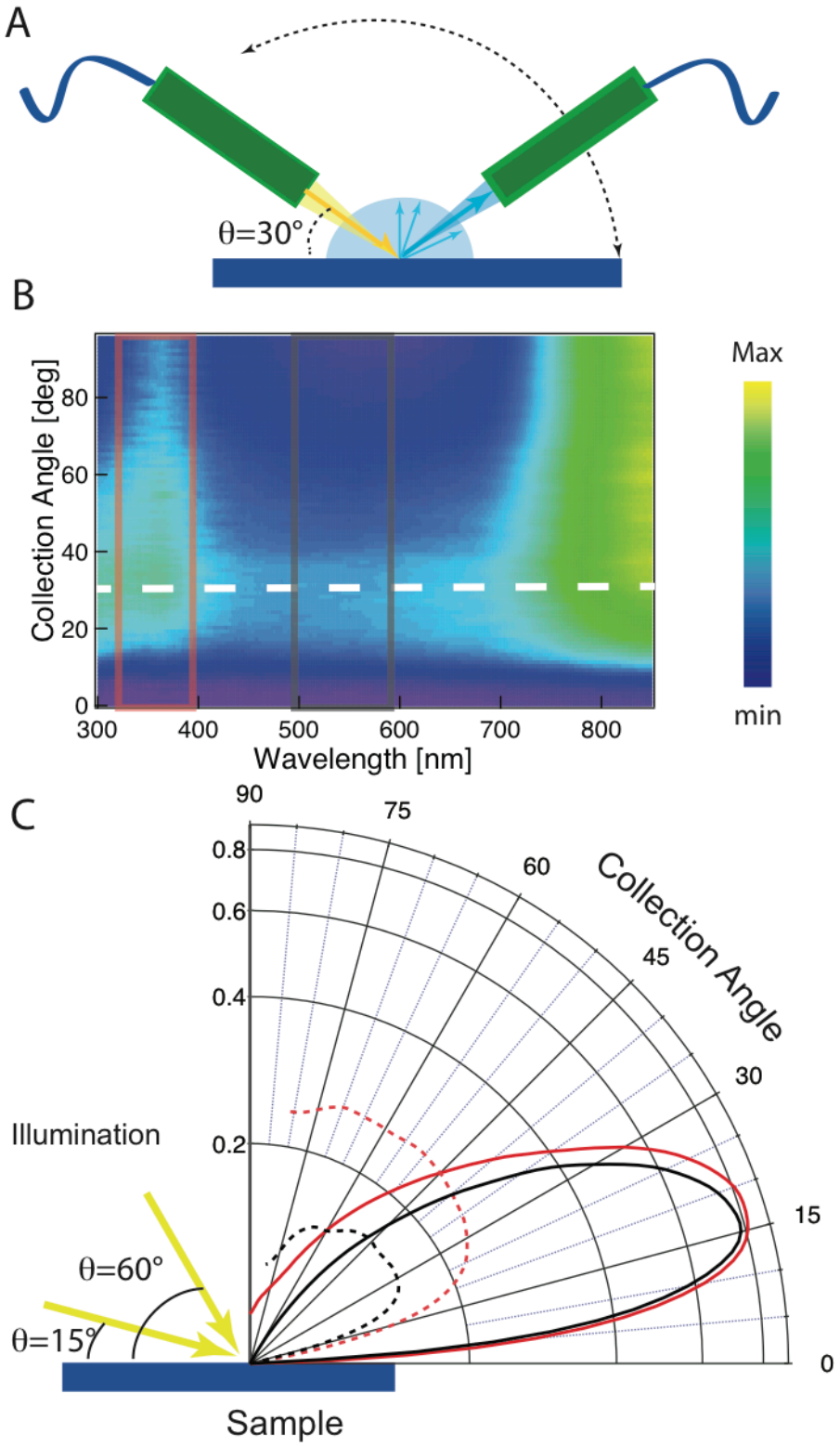

614

615 **Fig. 3** Optical characterization of the *Ophrys speculum* flower. A. Diagram of the goniometer

616 assembly. During measurements the illumination arm can be fixed at a definite angle (30° in

617 the diagram) and the collection arm is varied to collect the scattered light in the plane
618 perpendicular to the sample, as shown by the dotted black double-arrowed curve. B. Scattering
619 measurements from the speculum obtained with the configuration shown in A. The collection
620 angle is plotted on the Y axis and the wavelength on the X axis. The dotted white line
621 corresponds with the specular reflection direction, while the two coloured rectangles indicate
622 the regions in which we integrated the spectra for the analysis reported in C. C. Polar
623 scattering intensity distribution. The graph shows the integrated intensity as a function of the
624 illumination angle. To obtain the curves, we integrated the intensity of the reflected light in
625 two wavelength intervals: 300-400 nm (red lines) and 500–600 nm (black lines), for two
626 angles of collection for two contrasting incidence angles (15° incidence, shown as solid lines,
627 and 60° incidence, shown as dashed lines).

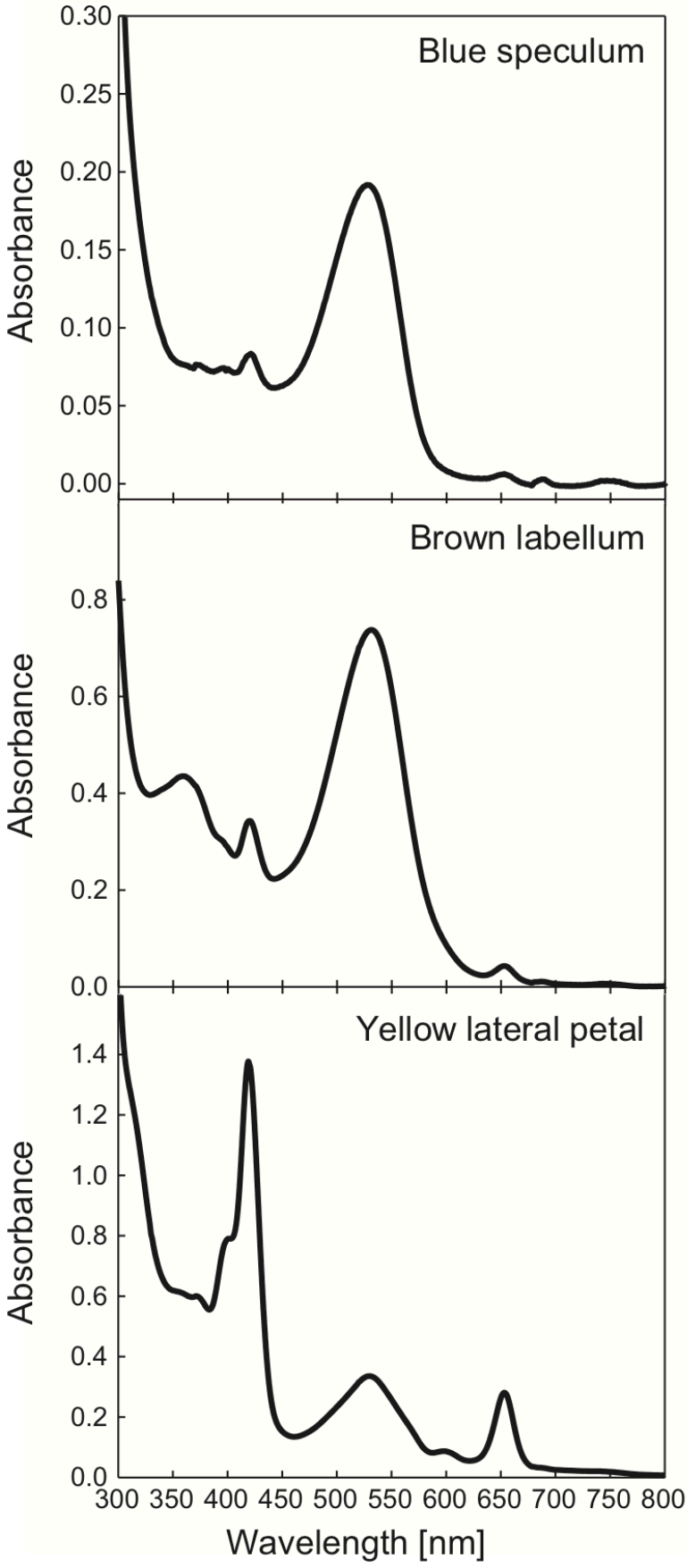
Blue speculum
Brown labellum
Yellow lateral petal
Absorbance
Absorbance
Absorbance
0.30
0.25
0.20
0.15
0.10
0.05
0.00
0.8
0.6
0.4
0.2
0.0
1.4
1.2
1.0
0.8
0.6
0.4
0.2
0.0
300 350 400 450 500 550 600 650 700 750 800
Wavelength [nm]

628

629 **Fig. 4** Absorbance spectra from crude solvent extracts (methanol with 1% HCl) of the blue
630 speculum, brown labellar margins and the yellow lateral petals of *Ophrys speculum* flowers.

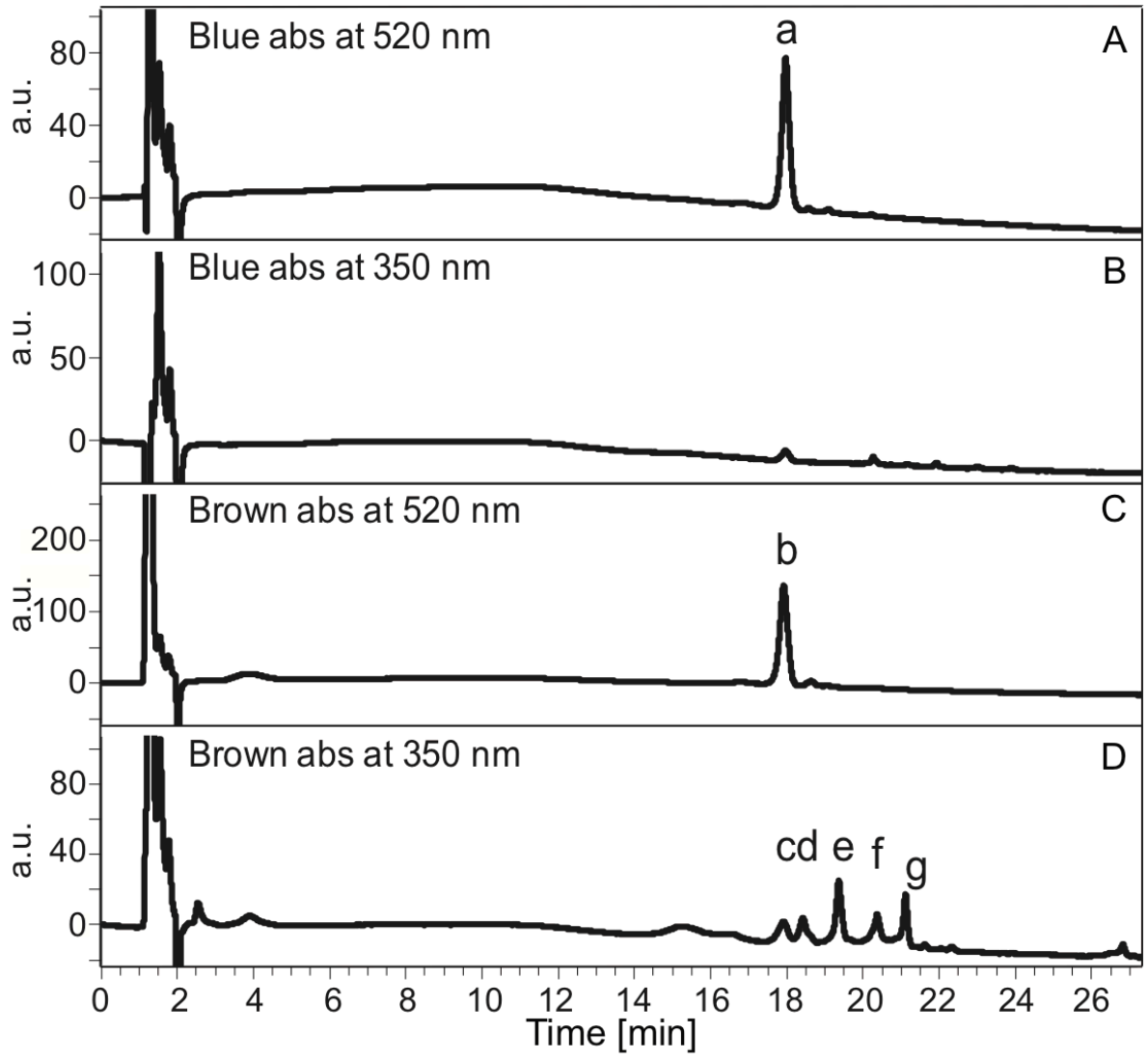

631

632 **Fig. 5** HPLC chromatograms (absorbance (abs) at 520 nm and 350 nm) of the crude extract
633 from the blue speculum and brown sections of the *Ophrys speculum* labellum. a, b, cyanidin 3-
634 (3"-malonylglucoside); d, delphinidin; c, e–g, flavonols.

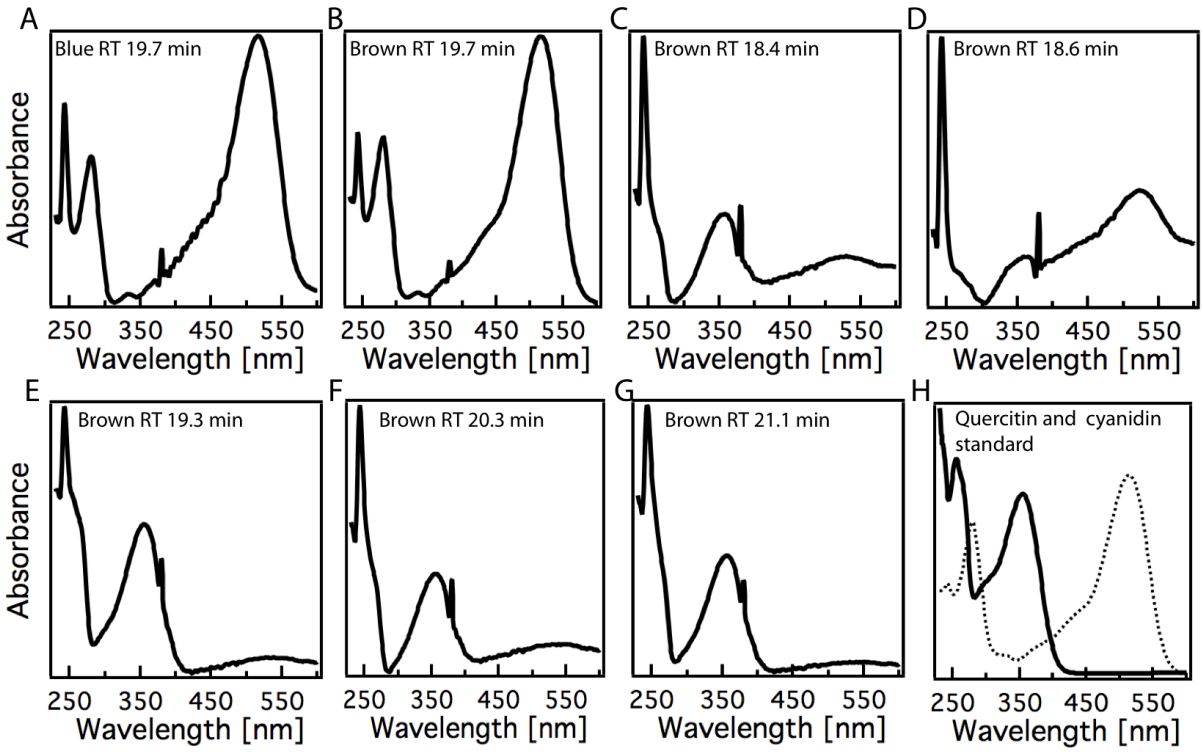

635

636 **Fig. 6** Analysis of the labellum pigments of *Ophrys speculum*. A. Absorption spectrum of the

637 metabolite from the blue speculum of *Ophrys speculum* eluting at 17.97 min. B–G.

638 Absorbance spectra of the metabolites from the peripheral brown section eluting at 17.97,

639 18.4, 18.6, 19.3, 20.3 and 21.1 min, respectively. H. Absorption spectrum of Quercitin-3-β-D-

640 glucoside (solid line) and cyanidin-3-O-glucoside (dashed line) standards.

641